Kinetic Treatment of Coupled Electron and Proton Transfer in Flash-Photolysis Experiments on Carbon Monoxide-Inhibited Mixed-Valence Cytochrome *c* Oxidase

A. I. Kotelnikov,[†] E. S. Medvedev,[†] D. M. Medvedev,[‡] and A. A. Stuchebrukhov*,[‡]

Department of Chemistry, University of California, Davis, California 95616, and Institute of Chemical Physics, Russian Academy of Sciences, 142432 Chernogolovka, Moscow, Russia

Received: January 3, 2001; In Final Form: March 23, 2001

Coupled electron and proton transfer observed in flow-flash experiments on CO-inhibited mixed-valence cytochrome *c* oxidase is discussed in terms of a model proposed by Brzezinski and co-workers [*J. Bioenerg. Biomembr*. **1998**, *30*, 99−107]. The model includes two redox states of the heme *a*/heme a_3 pair and two states, protonated and deprotonated, of a redox-linked group L, which is in contact with bulk solution via a proton conducting channel. The proton channel is represented by another protolytic group L′, which is in equilibrium with bulk solution, but not with group L. The theory reproduces the experimentally observed pH dependence of the slow kinetics of heme *a* reduction following dissociation of the enzyme−CO complex, and additionally predicts a pH dependence of the fast kinetics due to varying proton equilibrium between group L and bulk solution prior to dissociation. The rates of internal proton transfer between L and L′ in the reduced and oxidized states, and the bimolecular rate of protonation of L′ by bulk protons have been evaluated from the present theory and experimental data. The protonation rate of the group L in the reduced state of heme a_3 is $k_{on}^{red} = 10^4\ s^{-1}$. From the observed pH dependence of the rate constant for the slow kinetic phase of backward electron transfer the rate of L′ protonation is estimated to be $\kappa'_{on} = 5 \times 10^{11}\ M^{-1}\ s^{-1}$.

1. Introduction

Cytochrome *c* oxidase (CcO) performs an important function of translocating protons across the inner mitochondrial membrane, and thereby creating the membrane potential, by utilizing the energy released in dioxygen reduction.[1] Crystalline structures of CcO from bovine heart and some bacteria at high resolution have been recently obtained.[2−5] CcO performance under various conditions has been investigated in great detail (for recent reviews see refs 6−9). Theoretical studies of CcO include calculations of electrostatic potentials and interaction energies of ionizable groups of this enzyme,[10] molecular dynamics simulations,[11] ab initio studies of coupled electron−proton transfer,[12] proton conducting networks (proton wires),[13−17] electron tunneling pathways,[18] and others.

The development of a detailed kinetic model of the catalytic cycle is one of the major theoretical challenges. Such a model could be based on the assumption that the oxidase possesses a set of states with well-defined state energies and state-to-state rate constants. The specific CcO model could be characterized by parameters (energies and rate constants) found from experimental and calculated data. This program is far from being implemented in full yet. However, simpler models have been proposed for interpreting the results of particular experiments[19−25] that characterize different steps of the catalytic cycle of the enzyme. The development of simple models can be considered as a first step toward constructing a more complete model of the enzyme. In this paper we consider one of such models.

Recently, Brzezinski and co-workers[19−22] have measured the kinetics of electron transfer between hemes a_3 and *a*. Initially, the oxidase is fully oxidized except for the binuclear center held in the reduced state by carbon monoxide bound to it. The CcO−CO complex is dissociated by a laser flash, and subsequent changes in the populations of the redox states are monitored. The fast decay on the microsecond (μs) time scale is attributed to electron transfer that is not coupled to proton translocation, and the slow decay (the millisecond (ms) phase) is thought to be due to coupled electron−proton transfer. The authors proposed a simple model (see Figure 1), which includes two redox states of heme a_3 and two states (protonated and deprotonated) of a protonatable group L, which electrostatically interacts with heme a_3. This group communicates with bulk solution via a proton channel identified as the K-channel in ref 22. The proton channel is represented by a single protonatable group L′, which is in contact with both L and bulk solution and does not interact with L, nor with heme a_3. The following scheme is considered for proton transfer between bulk solution (BS) and group L,

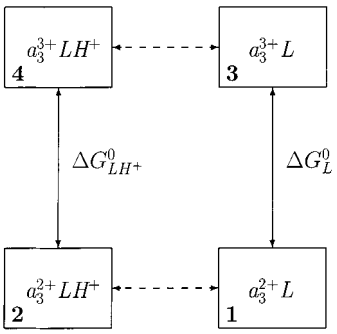

Figure 1. Four-state model by Brzezinski et al.[19−22] Solid lines, fast electron transfer. Dashed lines, slow proton transfer.

$$a_3^{2+/3+}\mathrm{L} \leftrightarrow \mathrm{L}' \leftrightarrow \mathrm{BS} \qquad (1.1)$$

Here, $a_3^{2+/3+}$L represents group L interacting with heme a_3.

[†] Russian Academy of Sciences.
[‡] University of California.

10.1021/jp010001t CCC: $20.00
Published on Web 05/16/2001

TABLE 1: Experimental and Theoretical Data from Refs 19−21

	$k_{on} - k_{off}$[a] (s^{-1})	k_{off} (s^{-1})	$\Delta G^0_{LH^+}$ (meV)	pH_{max}	$(\Delta P_{ms})_{max}$	pK' [b]	pK_{red}[c]	pK_{ox}[c]
bovine heart	1740 ± 120[d]	210 ± 80[d]	+42	9.4	0.21	7.7 ± 0.2[d]	9.7	8.5
Rhodobacter sphaeroides	2000[e]	≤150[e]	+10	9.7	0.19	8.7	10.3	9.1

[a] This difference is designated as k_{on} in refs 19−21. [b] Calculated by fitting the observed pH dependence of k_{obs} with eq 3.27 assuming fast equilibrium between L′ and bulk solution. [c] Calculated by fitting the observed pH dependence of the amplitude of the ms phase with an equation based on apparent redox potentials of heme a_3 in different protonation states of group L (see Discussion). [d] Experimental errors.[19] [e] No experimental errors are indicated, and only the upper limit for k_{off} is estimated.[20]

TABLE 2: Parameters Calculated in the Present Work

	bovine heart	*Rhodobacter sphaeroides*
pK_{red}	9.7	10.1
pK_{ox}	8.4	9.0
pK' [a]	8.2	8.2
ΔE_{a_3},[b] meV	78	62
$k_{12} = k^{red}_{on}$, s^{-1}	7660 ± 1590[c]	8940 ± 2070[d]
$k_{21} = k^{red}_{off}$, s^{-1}	200 ± 90[c]	120 ± 30[d]
$k_{34} = k^{ox}_{on}$, s^{-1}	610 ± 260[c]	1250 ± 270[d]
$k_{43} = k^{ox}_{off}$, s^{-1}	360 ± 230[c]	190 ± 40[d]

[a] Calculated from the on/off rate ratio, eq 3.30. [b] The interaction energy of the L group with the heme a_3 iron; see eq 3.11. [c] Uncertainties include experimental errors and the scatter of rate values, eq 4.5, introduced by our assumption of eq 4.2. [d] No experimental errors are included. The scatter of values is due to the assumption of eq 4.2.

Because of this interaction pK_a of this group depends on the redox state of heme a_3. The bulk solution is characterized by a given value of pH fixed by experimental conditions.

In this paper we present a detailed treatment of Brzezinski's group model. Our theory, which is based on kinetic equations for coupled electron−proton transfer, permits us to express both the rate constant and amplitude of the slow kinetic phase in terms of a common set of parameters of the model and to determine all the parameters from experimental data. The rates of protonation and deprotonation of the group L in two redox states of a_3, i.e., k^{red}_{on}, k^{red}_{off}, k^{ox}_{on}, and k^{ox}_{off}, obtained with this theory are shown in Table 2. In addition, the theory predicts that the amplitude of the fast phase must also depend on pH. The lack of such a dependence in experiment is discussed. These results are obtained under condition that L′ is in fast protonic equilibrium with bulk solution. The condition for maintaining this equilibrium in the slow kinetic phase is derived. An indication of a breakdown of the equilibrium is obtained from experimental data, and the rate constant for protonation of L′ from bulk solution is estimated. When the proton exchange between L′ and bulk solution is slower than between L′ and L, the slow kinetics is biphasic, with two rate constants being linearly dependent upon proton concentration.

2. Proton Transfer at a Given Heme a_3 Redox State

Kinetic equations for proton transfer in the scheme of eq 1.1 depend on the model of the proton channel. We will assume that protonation and deprotonation of L occur via exchange reactions with L′. On the other hand, L′ is treated as being immersed directly into bulk solution. The reaction scheme is

$$LH^+...L' \rightleftharpoons L...H^+L' \tag{2.1}$$

$$L'H^+ \rightleftharpoons L' + H^+ \tag{2.2}$$

Proton exchange between L′ and bulk solution, eq 2.2, is assumed to be very fast, so that equilibrium is maintained with the equilibrium constant

$$K' = \frac{k'_{off}}{\kappa'_{on}} \equiv 10^{-pK'} \tag{2.3}$$

where $k'_{off}$is the monomolecular rate constant of deprotonation and κ'_{on} is the bimolecular rate constant of protonation of L′. The fraction of the protonated groups L′ is

$$\alpha' \equiv \frac{[L'H^+]}{[L'H^+] + [L']} = \frac{1}{1 + 10^{pH-pK'}} \tag{2.4}$$

The assumption of fast L′−BS equilibrium will be discussed in sections 4 and 5.

The kinetic equation for reaction 2.1 with the reduced heme a_3 has the form

$$\frac{d}{dt}[a_3{}^{2+}LH^+] = -(1-\alpha')k^{red}_{off}[a_3{}^{2+}LH^+] + \alpha' k^{red}_{on}[a_3{}^{2+}L] \tag{2.5}$$

where the "off" and "on" rate constants are multiplied by fractions of deprotonated and protonated groups L′, respectively. The "on/off" rates depend on the redox state of heme a_3. At equilibrium

$$\frac{[a_3{}^{2+}L]}{[a_3{}^{2+}LH^+]} = \frac{(1-\alpha')k^{red}_{off}}{\alpha' k^{red}_{on}} \equiv 10^{pH-pK_{red}} \tag{2.6}$$

where pK_{red} is pK_a of L in the reduced state of a_3. The second relation is a consequence of thermodynamics that requires that equilibrium between L and bulk solution be independent of any intermediate L′. Then the ratio of the "on" and "off" rates is expressed in terms of the difference between p*K*'s of L and L′,[26]

$$\frac{k^{red}_{off}}{k^{red}_{on}} = 10^{pK'-pK_{red}} \tag{2.7}$$

The fraction of protonated groups L at the reduced state of heme a_3,

$$\alpha_{red} = \frac{1}{1 + 10^{pH-pK_{red}}} \tag{2.8}$$

is the same as if L were immersed directly into bulk solution. Equations 2.5−2.8 are written similarly for the oxidized state $a_3{}^{3+}$.

3. Kinetic Equations for Coupled Electron−Proton Transfer

In Figure 1 the numbering of states is indicated. The scheme of Figure 1 does not account for electron flow from heme *a* to the Cu_A center since the electron backflow observed in flow-flash experiments on the CO-inhibited CcO does not exceed 10%.[20]

The kinetic equations are written for the relative populations,

$$P_1 = \frac{[a_3{}^{2+}\mathrm{L}]}{N} \qquad P_2 = \frac{[a_3{}^{2+}\mathrm{LH}^+]}{N} \qquad P_3 = \frac{[a_3{}^{3+}\mathrm{L}]}{N}$$

$$P_4 = \frac{[a_3{}^{3+}\mathrm{LH}^+]}{N}$$

$$P_1 + P_2 + P_3 + P_4 = 1 \tag{3.1}$$

where N is the total concentration of the active enzyme−CO complexes. For brevity, proton-transfer rate constants at a given redox state are denoted as

$$k_{12} = k_{\mathrm{on}}^{\mathrm{red}} \qquad k_{21} = k_{\mathrm{off}}^{\mathrm{red}} \qquad k_{34} = k_{\mathrm{on}}^{\mathrm{ox}} \qquad k_{43} = k_{\mathrm{off}}^{\mathrm{ox}} \tag{3.2}$$

Electron-transfer rate constants at a given protonation state are k_{13}, k_{31}, k_{24}, and k_{42}. Using eq 2.5, we obtain the kinetic equations in the form

$$\dot{P}_1 = -(\alpha' k_{12} + k_{13})P_1 + (1-\alpha')k_{21}P_2 + k_{31}P_3 \tag{3.3}$$

$$\dot{P}_2 = \alpha' k_{12}P_1 - [(1-\alpha')k_{21} + k_{24}]P_2 + k_{42}P_4 \tag{3.4}$$

$$\dot{P}_3 = k_{13}P_1 - (k_{31} + \alpha' k_{34})P_3 + (1-\alpha')k_{43}P_4 \tag{3.5}$$

$$\dot{P}_4 = k_{24}P_2 + \alpha' k_{34}P_3 - [k_{42} + (1-\alpha')k_{43}]P_4 \tag{3.6}$$

The electron-transfer rate constants obey the following thermodynamic relations:

$$K_{13} \equiv \frac{k_{13}}{k_{31}} = \exp\left(-\frac{\Delta G_{\mathrm{L}}^0}{k_{\mathrm{B}}T}\right) \tag{3.7}$$

$$\Delta G_{\mathrm{L}}^0 = E_{a_3\mathrm{L}} - E_a \tag{3.8}$$

$$K_{24} \equiv \frac{k_{24}}{k_{42}} = \exp\left(-\frac{\Delta G_{\mathrm{LH}^+}^0}{k_{\mathrm{B}}T}\right) \tag{3.9}$$

$$\Delta G^0_{\mathrm{LH}^+} = E_{a_3\mathrm{LH}^+} - E_a \tag{3.10}$$

where E_a is the reduction potential of heme a and $E_{a_3\mathrm{LH}^+}$ and $E_{a_3\mathrm{L}}$ are the redox potentials of heme a_3 for protonated and deprotonated states of group L, respectively. The change in the reduction potential of heme a_3 upon protonation of L is expressed in terms of the change in pK_a of L,[20]

$$\Delta E_{a_3} \equiv E_{a_3\mathrm{LH}^+} - E_{a_3\mathrm{L}} = k_{\mathrm{B}}T\ln(10)\Delta\mathrm{p}K \tag{3.11}$$

$$\Delta\mathrm{p}K = \mathrm{p}K_{\mathrm{red}} - \mathrm{p}K_{\mathrm{ox}} \tag{3.12}$$

The proton-transfer rate constants obey the relations which stem from eq 2.7,

$$K_{12} \equiv \frac{k_{12}}{k_{21}} = 10^{\mathrm{p}K_{\mathrm{red}} - \mathrm{p}K'} \tag{3.13}$$

$$K_{34} \equiv \frac{k_{34}}{k_{43}} = 10^{\mathrm{p}K_{\mathrm{ox}} - \mathrm{p}K'} \tag{3.14}$$

From eqs 3.7−3.14 we obtain the relations between the equilibrium constants,

$$\frac{K_{13}}{K_{24}} = \frac{K_{12}}{K_{34}} = 10^{\Delta\mathrm{p}K} \tag{3.15}$$

Initially, CO is bound to the binuclear center, so that heme a_3 is fixed at its reduced state, $a_3{}^{2+}$, whereas heme a is in the oxidized state, a^{3+}. At times $t < 0$, no electron transfer occurs and proton equilibrium is established. It is assumed that the presence of CO does not affect pK_a of L due to a large separation (5−10 Å, as estimated in ref 21). Then, the initial conditions at $t = 0$ are

$$P_1^{(0)} = \frac{1-\alpha'}{1-\alpha'+\alpha' K_{12}} = 1-\alpha \qquad P_3^{(0)} = 0 \tag{3.16}$$

$$P_2^{(0)} = \frac{\alpha' K_{12}}{1-\alpha'+\alpha' K_{12}} = \alpha \qquad P_4^{(0)} = 0 \tag{3.17}$$

where, for brevity, α stands for α_{red} in eq 2.8, and eqs 2.4 and 3.13 were used.

After CO is flashed out, the $1 \leftrightarrow 3$ and $2 \leftrightarrow 4$ electron-transfer channels become open. They govern the fast (μs) phase of the observed kinetics of heme a reduction. The difference in the electron and proton-transfer rate constants is about 3 orders of magnitude. Therefore, we can neglect protonic transitions in the fast phase and solve eqs 3.3−3.6 with the initial conditions (3.16) and (3.17). After completion of the fast phase and before beginning the slow phase, at a moment t_1 such that $k_{12}{}^{-1} \gg t_1 \gg k_{13}{}^{-1}$, we obtain the following populations:

$$P_1^{(1)} = \frac{1-\alpha}{1+K_{13}} \tag{3.18}$$

$$P_2^{(1)} = \frac{\alpha}{1+K_{24}} \tag{3.19}$$

$$P_3^{(1)} = \frac{(1-\alpha)K_{13}}{1+K_{13}} \tag{3.20}$$

$$P_4^{(1)} = \frac{\alpha K_{24}}{1+K_{24}} \tag{3.21}$$

The reduction degree of heme a equals to the population of the $a_3{}^{3+}$ state,

$$P^{(1)}(a_3{}^{3+}) = P_3^{(1)} + P_4^{(1)} \tag{3.22}$$

The change of the degree of the heme a_3 oxidation during the μs phase, i.e., the observed amplitude of the fast kinetic phase, is

$$\Delta P_{\mu\mathrm{s}} = P^{(1)}(a_3{}^{3+}) - P^{(0)}(a_3{}^{3+}) = \frac{(1-\alpha)K_{13}}{1+K_{13}} + \frac{\alpha K_{24}}{1+K_{24}} \tag{3.23}$$

At $t > t_1$ the slow (ms) phase develops. The relevant quantities to describe the slow kinetics are populations of the deprotonated and protonated states, $P_{\mathrm{L}} = P_1 + P_3$ and $P_{\mathrm{LH}^+} = P_2 + P_4$, respectively. Using the relations established in the fast phase, $P_3 = K_{13}P_1$ and $P_4 = K_{24}P_2$, which are approximately obeyed in the slow phase as well, we obtain from the sum of eqs 3.3 and 3.5

$$\dot{P}_L = -\alpha' k_{on} P_L + (1-\alpha') k_{off} P_{LH^+} \quad (3.24)$$

$$k_{on} = \frac{k_{12} + k_{34}K_{13}}{1+K_{13}} = \frac{K_{12}(k_{21} + k_{43}K_{24})}{1+K_{13}} \quad (3.25)$$

$$k_{off} = \frac{k_{21} + k_{43}K_{24}}{1+K_{24}} \quad (3.26)$$

where eqs 3.13−3.15 were used. The populations are normalized according to eq 3.1, $P_L + P_{LH^+} = 1$. The observed slow decay rate constant is

$$k_{obs} = \alpha' k_{on} + (1-\alpha') k_{off} \quad (3.27)$$

Thus, eq 3.24 predicts a single-exponential decay in the ms phase with the rate 3.27. After completion of the slow decay, at a moment $t_2 \gg k_{obs}^{-1}$, the populations of the reduced heme a_3 states are

$$P_1^{(2)} = \frac{(1-\alpha')k_{off}}{k_{obs}(1+K_{13})} \quad (3.28)$$

$$P_2^{(2)} = \frac{\alpha' k_{on}}{k_{obs}(1+K_{24})} \quad (3.29)$$

These populations are in fact independent of the intermediate group L′. To show this explicitly, we express the ratio of the "on" and "off" rates according to eqs 3.25 and 3.26 as

$$\frac{k_{on}}{k_{off}} = \xi K_{12} \quad (3.30)$$

$$\xi = \frac{1-K_{24}}{1+K_{13}} = \frac{1+K_{24}}{1+K_{24}10^{\Delta pK}} \quad (3.31)$$

Then, eqs 3.28 and 3.29 are rewritten in the form

$$P_1^{(2)} = \frac{1-\alpha}{(1+K_{13})(1-\alpha+\alpha\xi)}$$

$$P_2^{(2)} = \frac{\alpha}{(1+K_{13})(1-\alpha+\alpha\xi)} \quad (3.32)$$

independent of L′. It is worthwhile to note that in general the state-to-state rate constants k_{21} and k_{43} cannot be expressed individually in terms of the measured "on" and "off" rates since the on/off ratio (3.30) is independent of the state-to-state rates. Yet, these constants can be reasonably estimated from experimental data (see section 4).

The degree of heme *a* reduction at moment t_2 is equal to the population of the oxidized heme a_3 states,

$$P^{(2)}(a_3{}^{3+}) = 1 - P_1^{(2)} - P_2^{(2)} = \frac{K_{13}}{1+K_{13}} - \frac{(1-\xi)\alpha}{(1+K_{13})(1-\alpha+\alpha\xi)} \quad (3.33)$$

The same quantity at moment t_1 is given by eqs 3.20−3.22,

$$P^{(1)}(a_3{}^{3+}) = \frac{K_{13}}{1+K_{13}} - \frac{1-\xi}{\xi}\frac{\alpha}{1+K_{13}} \quad (3.34)$$

The change of the degree of the heme a_3 oxidation during the ms phase, i.e., the observed amplitude of the slow kinetic phase, is

$$\Delta P_{ms} = P^{(2)}(a_3{}^{3+}) - P^{(1)}(a_3{}^{3+}) = \frac{(1-\xi)^2\alpha(1-\alpha)}{(1+K_{24})(1-\alpha+\alpha\xi)} \quad (3.35)$$

Equation 3.35 predicts that the slow phase disappears when electron transfer is decoupled from proton transfer. In this case $\Delta pK = 0$ and the electron-transfer rate constants are independent of the protonation state of L, i.e., $K_{13} = K_{24}$ and $\xi = 1$. The pH dependence of ΔP_{ms} is explicitly governed by α. The amplitude of the slow phase disappears in both low and high pH limits since L remains fully protonated or deprotonated in the course of experiment. The maximum occurs at

$$pH_{max} = pK_{red} + 0.5 \log \xi \quad (3.36)$$

$$(\Delta P_{ms})_{max} = \frac{(1-\sqrt{\xi})^2}{1+K_{24}} \quad (3.37)$$

We note that the amplitude of the fast phase given by eq 3.23 also depends on pH, but in a different manner. Since $\Delta pK > 0$ and $E_{a_3LH^+} > E_a > E_{a_3L}$,[20] one has $K_{13} > 1 > K_{24}$,and $\Delta P_{\mu s}$ increases with increasing pH.

4. Results

Here, we will calculate the parameters of the model and compare the present theory with experimental and theoretical results of refs 19−21. Experimental values of k_{on}, k_{off}, $\Delta G^0_{LH^+}$, pH_{max}, and $(\Delta P_{ms})_{max}$ for CcO from bovine heart and *Rhodobacter sphaeroides* are shown in Table 1. Our theoretical results are summarized in Table 2 and discussed below in this section.

The rate ratio k_{on}/k_{off}, the equilibrium constant K_{24} at $T =$ 295 K, and ξ are directly calculated using the data of Table 1 and eqs 3.9 and 3.37. Then K_{12}, K_{13}, ΔpK, and ΔE_{a_3} are found from eqs 3.30, 3.31, and 3.11. Further, pK_{red} and pK_{ox} are calculated by eqs 3.36 and 3.12. Finally, pK' is found from eq 3.13. The calculated parameters for bovine heart enzyme are as follows (the parameters for bacterial enzyme are given in parentheses): $k_{on}/k_{off} = 9.3$ (14.3), $K_{24} = 0.19$ (0.67), $\xi = 0.25$ (0.19), $K_{12} = 37$ (75), $K_{13} = 3.8$ (7.8), $\Delta pK = 1.3$ (1.1). The values of pK's and ΔE_{a_3} are shown in Table 2.

The pH dependence of the amplitude of the slow phase in CcO from bovine heart calculated by eq 3.35 with the above parameters is given in Figure 2 along with the experimental data and the theoretical curve from Figure 3B of ref 21.

The present theory predicts a pH dependence of the degree of heme a_3 oxidation in the fast phase as well. Indeed, proton equilibration occurs prior to the flash, resulting in pH-dependent initial populations of the protonated and deprotonated states which thereafter decay with different electron-transfer rates. This fact is described by our eqs 3.16 and 3.17. In ref 20 the second term of eq 16 also represents the pH-dependent $\Delta P_{\mu s}$. In our notations it reads

$$\Delta P_{\mu s} = \frac{1}{1+K_{24}{}^{-1}10^{(\alpha-1)\Delta pK}} \quad (4.1)$$

The amplitude of the fast phase calculated by eqs 3.23 and 4.1 is shown in Figure 3.

Next we will estimate the rate constants (3.2) for protonation and deprotonation of group L in the reduced and oxidized states of heme a_3. These four state-to-state constants are not measured

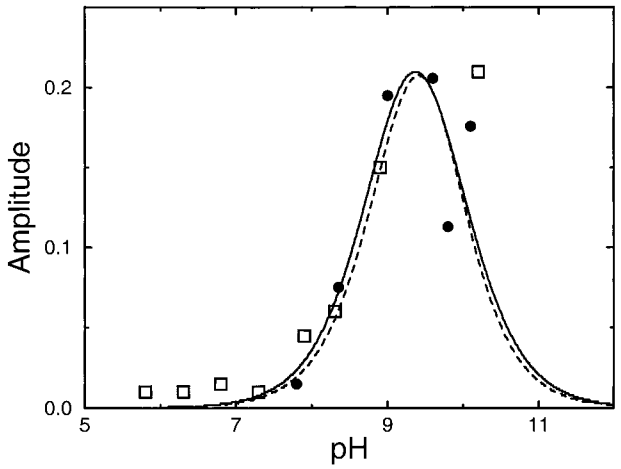

Figure 2. Amplitude of the slow phase in CcO from bovine heart. Solid line, eq 3.35 with parameters from Table 2. Squares and dots, experimental data from ref 21. Dashed line, theoretical curve from ref 21.

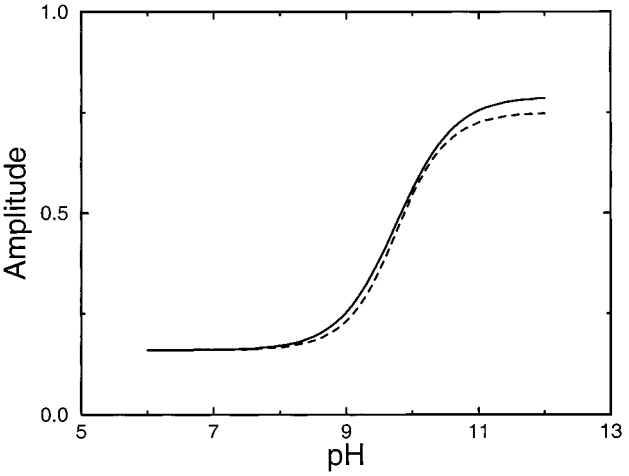

Figure 3. Amplitude of the fast phase in CcO from bovine heart. Solid line, eq 3.23 with parameters from Table 2. Dashed line, eq 4.1 with parameters from Table 1.

individually. Rather, only two average constants k_{on} and k_{off}, eqs 3.25 and 3.26, representing the state-to-state constants weighted with equilibrium constants for electron-transfer reactions are obtained in experiment. With equilibrium constants K_{12} and K_{34}, eqs 3.13 and 3.14, we have only three independent equations to find the above four unknowns. Yet, we can get reasonable estimates by assuming that deprotonation is faster and protonation is slower in the oxidized state than in the reduced state of heme a_3. This is illustrated by the energy diagram of Figure 4 where $\Delta E^{\dagger}_{a_3}$ and ΔE_{a_3} are energy increments of the transition state and the protonated state of L, respectively, due to electrostatic repulsion between proton and heme iron ion, which is stronger in the oxidized state of the heme. One has $\Delta E_{a_3} > \Delta E^{\dagger}_{a_3}$ since the proton is closer to the heme iron in the LH^+ state than in the transition state. Further, if we assume that the distance between the position of the proton in the LH^+ state and that in the transition state $(L...H^+)^{\dagger}$ is 1−2 Å, then from Figure 6 of ref 21 we can estimate that the decrease of the electrostatic energy when the proton moves from L to the transition state does not exceed 0.4 p*K* units ≈ 24 meV. Hence, we obtain the following estimate,

$$\Delta E_{a_3} - 24\ \text{meV} < \Delta E^{\dagger}_{a_3} < \Delta E_{a_3} \tag{4.2}$$

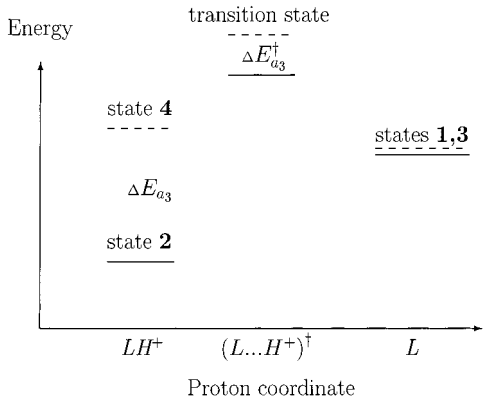

Figure 4. Energy diagram for proton movement in the reduced (solid lines) and oxidized (dashed lines) states of heme a_3.

Using ΔE_{a_3} from Table 2, we obtain the values of $\Delta E^{\dagger}_{a_3} = 66 \pm 12$ meV for bovine enzyme and 50 ± 12 meV for bacterial enzyme. From Figure 4 one can see that the rate constants obey the relation

$$\frac{k_{43}}{k_{21}} = \exp\left(\frac{\Delta E_{a_3} - \Delta E^{\dagger}_{a_3}}{k_B T}\right) \tag{4.3}$$

Using inequality (4.2), we obtain the following restriction onto the rate constants,

$$1 < \frac{k_{43}}{k_{21}} < 10^{0.4} = 2.5 \tag{4.4}$$

This additional condition helps us find all four constants. From eqs 3.26 and 4.4 we obtain

$$\frac{1 + K_{24}}{1 + 2.5K_{24}} < \frac{k_{21}}{k_{off}} < 1 \tag{4.5}$$

$$\frac{k_{43}}{k_{off}} = 1 + \frac{1}{K_{24}}\left(1 - \frac{k_{21}}{k_{off}}\right)$$

Then, k_{12} and k_{34} are calculated from eqs 3.13, 3.14, and 3.30, which are rewritten as

$$k_{12} = \frac{k_{on}}{\xi}\frac{k_{21}}{k_{off}}$$

$$k_{34} = \frac{k_{on}}{\xi}\frac{k_{43}}{k_{off}}10^{-\Delta pK}$$

For bovine heart enzyme, using k_{off} from Table 1 and K_{24} calculated at the beginning of this section, we obtain $105\ s^{-1} < k_{21} < 290\ s^{-1}$ or $k_{21} = 200 \pm 90\ s^{-1}$. The uncertainty includes both the scatter of values, eq 4.5, owing to our assumed scatter in $\Delta E^{\dagger}_{a_3}$ values, eq 4.2, and the experimental errors in the measured values of k_{on} and k_{off}. For bacterial enzyme no experimental uncertainty was indicated in ref 20; therefore we treated k_{on} and k_{off} of Table 1 as exact. The calculated rate constants are given in Table 2.

Finally, we studied the slow kinetics in the case where no L′−BS equilibrium is established. Then, all four protonation states of L and L′ have to be considered according to the reaction scheme in eqs 2.1 and 2.2. The kinetics depends on two pairs of rate constants, i.e., k'_{off} and κ'_{on} governing proton exchange between L′ and bulk solution, and the constants k_{on} and k_{off} given by eqs 3.25 and 3.26, which govern the L ↔ L′ proton exchange.

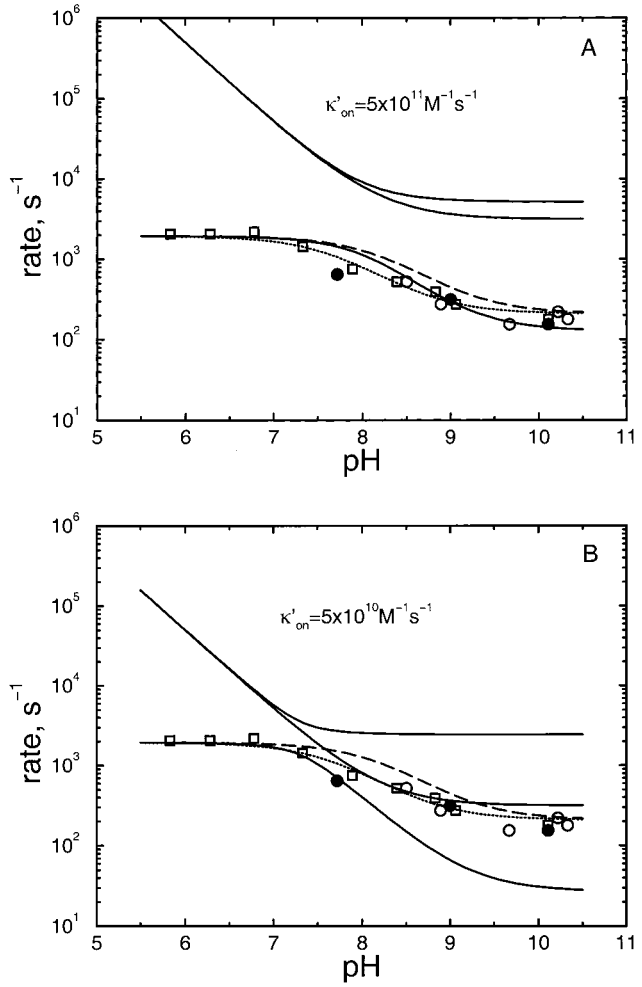

Figure 5. pH-dependent rate constants for proton movement in bovine heart enzyme. Panel A, high combination rate $\kappa'_{on} = 5 \times 10^{11}$ M^{-1} s^{-1}. Panel B, low combination rate $\kappa'_{on} = 5 \times 10^{10}$ M^{-1} s^{-1}. Full lines, three roots of the secular equation for the reaction scheme of eqs 2.1 and 2.2. Dashed line, eq 3.27 with p$K' = 8.2$. Dotted line, eq 3.27 with p$K' = 7.7$. Squares and circles, experimental data from Figure 3A of ref 21.

By solving the secular equation we calculated three rate constants for bovine heart enzyme shown by full lines in Figure 5.We found that at high combination rate, $\kappa'_{on} \geq 10^{12}$ M^{-1} s^{-1}, two higher rates represent the kinetics of fast L′−BS equilibration, whereas the lowest rate relates to the slow kinetics of the L′−L proton exchange (not shown). The slow kinetics is monophasic and its rate constant shows a sigmoidal pH dependence, as described by eq 3.27. On a limited pH interval, e.g., pH 8−10, this dependence may appear as a linear one with the slope at the middle point of

$$\mathrm{d}\log k_{obs}/\mathrm{dpH} = -\frac{1}{2}\left(\frac{k_{on} - k_{off}}{k_{on} + k_{off}}\right) \approx -0.5$$

since $k_{on} \gg k_{off}$ (see Table 1). In the opposite limit of low combination rates, $\kappa'_{on} \leq 3 \times 10^{11}$ M^{-1} s^{-1}, the slow kinetics is biphasic and two rates are linearly dependent on the proton concentration, with d log k_{obs}/dpH $= -1$ at pH < pK' (not shown). Two patterns of nonequilibrium behavior are shown in Figure 5, where points are experimental data from Figure 3A of ref 21, and dashed and dotted lines are calculated by eq 3.27 with p$K' = 8.2$ and 7.7, respectively. The value of p$K' = 8.2$ was calculated by us from the rate data (see Table 2), whereas p$K' = 7.7$ was suggested in ref 21 as the best fit of eq 3.27 to the experimental data assuming full L′−BS equilibrium (see Table 1). If this discrepancy between the two values of pK' is significant, it can be explained in the present theory by a deviation from the full L′−BS equilibrium in the course of the slow kinetic phase, as shown in Figure 5A for $\kappa'_{on} = 5 \times 10^{11}$ M^{-1} s^{-1}. The slow rate (the bottom full line) is smaller, and it fits experimental data better than the rate under full L′−BS equilibrium (dashed line). When κ'_{on} is further decreased below 3×10^{11} M^{-1} s^{-1}, the L′−BS equilibrium does not exist anymore, as illustrated in Figure 5B for $\kappa'_{on} = 5 \times 10^{10}$ M^{-1} s^{-1}, which is close to the diffusion-controlled limit of $(2-4) \times 10^{10}$ M^{-1} s^{-1}.[27] The kinetics is biphasic and logarithm of the slower rate shows a linear dependence upon pH at pH 7−9. It strongly deviates from the experimental data, and its pH dependence shows a slope of −1 characteristic of the diffusion-controlled protonation kinetics.

5. Discussion

Equation 3.27 for the rate constant of the slow phase rewritten in the form

$$k_{obs} = \alpha'(k_{on} - k_{off}) + k_{off} \qquad (5.1)$$

is similar to that proposed in refs 19−21 where $k_{on} - k_{off}$ in the first term is replaced with k_{on}. It predicts the same pH dependence, with saturation at both low and high pH. However, the meaning of the parameters k_{on} and k_{off} is different. Apart from a numerical change due to the above replacement, our eqs 3.25 and 3.26 explicitly take into account the dependence of the proton-transfer rates on the redox state of heme a_3. The present theory enabled us to estimate these redox-dependent rates using the experimental data. The results are shown in Table 2. It is worthwhile to note that the measured rate of proton transfer along the gramicidin channel across biomembranes is 6.5×10^4 s^{-1}, and that the same mechanism is assumed to operate in other proton-transporting proteins including CcO.[28] Our result for protonation of L (proton transfer in forward direction from bulk to the active site), $(8 - 9) \times 10^3$ s^{-1}, compares well with the above-cited rate.

We also emphasize that eqs 3.27 and 5.1 are only valid on condition of fast equilibrium between L′ and bulk solution, and this condition was specified quantitatively. We estimated that it is fulfilled when $\kappa'_{on} > 10^{12}$ M^{-1} s^{-1}, where κ'_{on} is the bimolecular rate constant for protonation of the proton channel from bulk solution, and it is broken down when $\kappa'_{on} < 3 \times 10^{11}$ M^{-1} s^{-1}. From comparison with experiment, which shows some deviation from the full equilibrium, we estimated $\kappa'_{on} = 5 \times 10^{11}$ M^{-1} s^{-1}. This value is significantly higher than the determined rate constants for proton binding to macromolecular structures, $(2-6) \times 10^{10}$ M^{-1} s^{-1},[28] which are in the range of diffusion-controlled reactions. Yet, proton binding can be accelerated due to proton-collecting antennas[28] and fast proton translocation via networks of hydrogen bonds.

We can formulate a criterion for the fast equilibrium and for the lack thereof based on the pH dependence of log k_{obs}. This dependence is linear for low combination rate κ'_{on}(no equilibrium) with the slope of −1 at pH < pK' since in this case $k_{obs} \approx \kappa'_{on}[H^+]$. On the other hand, in the case of fast equilibrium (high combination rate) the pH dependence is sigmoidal, but it may appear as linear in a limited interval of pH around the midpoint, with twice as low the slope of −0.5. For instance, in the stopped-flow experiment by Verkhovsky et al.[25] on the reaction of pulsed oxidized CcO with reduced ruthenium hexaammine a biphasic behavior was observed with linear

dependence of two rates upon pH in the range of pH 7−9. The slope of both graphs is close to −0.5, which testifies the fast L′−BS equilibrium, whereas the biphasicity originates from other reasons than the lack of L′−BS equilibrium.

Next we discuss the amplitudes of the kinetic phases. We note that the equations for the amplitudes are independent of the actual kinetics, i.e., whether L′ is or is not in fast equilibrium with solution, since the amplitudes depend on equilibrium or quasiequilibrium states of the system. Our eq 3.35 for the amplitude of the slow phase is essentially different from eq 16 of ref 20, and the same is true for the amplitude of the fast phase. For example, the amplitude of the fast phase is a linear function of α in eq 3.23, whereas it is an exponential function in eq 4.1. This is because Ädelroth et al. considered electron-transfer equilibrium between two redox states with apparent reduction potentials whereas we took into account individual contributions of all four participating states. As a result, our eq 3.35 depends on the equilibrium constants K_{13} and K_{24} for individual electron transfers with deprotonated and protonated L group, respectively, rather than on the averaged equilibrium constants derived from the apparent potentials. The other important feature is that the theory of ref 20 does not provide any relation between the amplitude and the rate of the slow phase, while both quantities describe one and the same process. In contrast, the present theory shows this relation explicitly since eq 3.30 for the on/off rate ratio and eq 3.35 for the amplitude depend on the common parameter ξ.

Equation 3.30 was used to calculate the pK' values from the rate data (Table 2) and compare them with the results of refs 19 and 20 obtained from a fit to the observed rate assuming fast equilibrium between L′ and solution (Table 1). The difference between two values can be explained by a deviation from fast equilibrium, as explained above. Yet the difference of 0.5 in the pK' values is not very large as compared to the uncertainty involved, to make a definite conclusion. The second result of this analysis is our finding that the equilibrium is definitely not maintained at a combination rate of slower than 3×10^{11} M^{-1} s^{-1}. Since the equilibrium, or nearly equilibrium, does exist in the flow-flash experiment under study, we can conclude that the combination rate is significantly higher, approaching 10^{12} M^{-1} s^{-1}.

It is seen that both theories give nearly identical pH dependencies of the amplitudes of the slow and fast phases. Similar results are obtained for bacterial CcO (not shown). Our values for pKs of L in Table 2 are nearly the same as those obtained in refs 20 and 21 despite the fact that our equations are analytically very different from those of ref 20. However, this difference is expected to manifest numerically at higher ΔpK, e.g., like those found in ref 29. Higher ΔpK are expected if a water molecule bound to the reduced binuclear center plays a role of the L group in its protonated state.[19]

The present model accounts for a single protonatable group L in a vicinity of the binuclear center. In fact, there is a second proton channel, the D-channel, redox-linked to heme *a*, and a channel for outgoing protons, as well as several protonatable groups at each redox site (see, e.g., refs 6−10, 22, and 29−32 and references therein). Papa et al.[29] identified two groups interacting with heme a_3, one interacting with heme *a*, and one with Cu_B. The pKs of the groups near heme a_3 are equal to 7 in the oxidized state and ≥12 in the reduced state of heme a_3, which are far from the values found in ref 20 and in the present work. One of these groups might be a water molecule mentioned above. With a high value of pK_{red} this L group will always be protonated when heme a_3 is reduced, which will result in a pH-independent amplitude of the fast phase in accordance with the experiment in refs 19−22. However, our theory predicts that in this case the amplitude of the slow phase will be monotonically increasing with pH whereas the experiment shows a maximum (see Figure 2). The experimentally observed independence of the fast phase upon pH may indicate an inhomogeneous decay. For instance, a fraction of the active enzyme−CO complexes may have a water molecule near the binuclear center that could provide a large pH-independent contribution to the fast kinetic phase whereas another population with no water molecule at the binuclear center would contribute to the descending branch of the amplitude of the slow phase. Another possibility is that a significant fraction of enzyme molecules may have had their proton channels impaired, so that their L's are decoupled from the bulk solution and always remain in a given state of protonation. Then, the fast decay is mostly due to this population of enzymes, whereas the contribution of the "normal" enzymes is seen only in the slow phase. On the other hand, we note that the appearance of the maximum in the amplitude of the slow phase does not seem to be very convincing, especially for bacterial enzyme. If the maximum is an artifact, a water molecule will be a good candidate for the L group responsible for the observed pH dependence of the slow phase.

A few comments are also due to the following features of the present model.

(i) It is assumed that CO locks heme a_3 in its reduced state, while there are data indicating that a_3^{2+}−CO complex can be oxidized by ferricytochrome.[33] This means that in the course of preparation of the mixed-valence enzyme−CO complex a fraction of the complexes is destroyed at the stage of oxidation. The total concentration of the survived complexes showing up in a flash-photolysis experiment depends on experimental conditions, in particular on pH. This circumstance does not influence our equations because all kinetic curves are normalized to the total concentration of the available complexes.

(ii) In addition to the centers represented in Figure 1, there are two copper centers that are ignored in the present model. This is justified because Cu_B always remains in its reduced state and the electron flow to Cu_A does not exceed 10% in these experiments.[20]

(iii) The pK of the L group is assumed to be unaffected by CO unbinding from a_3. If L is located far away from a_3, so that ΔpK due to a change in the redox state of a_3 is small, then this is justified since CO does not move a long way from the binuclear center when flashed out of it. Instead, CO resides in a vicinity of the center because its rebinding starts very shortly after the coupled electron and proton transfer is completed. However, the pK of L can be affected when L is a ligand to a_3, as discussed above in this section.

(iv) The present model does not exclude the possibility that the event called here an "electron transfer" is in fact concerted electron plus proton transfer in which both electron and proton are translocated rapidly with the same rate. Our equations apply to this case as well.

(v) The redox cooperativity is usually an important factor affecting the redox potentials of the participating centers. However, in the experiments under study, only a single electron is translocated between the centers whereas the second one resides permanently on Cu_B. Therefore, there is no change in the redox potentials in the course of the back electron flow from the binuclear center.

Acknowledgment. We appreciate helpful discussions with P. Brzezinski and M. Verkhovsky. This work has been supported

by research grants from the National Institutes of Health (GM54052-02), NIH Fogarty International Center (1 R03 TW00954-01), INTAS (99-00281), and the Russian Foundation for Basic Research (98-03-33155,98-04-48955). A.A.S. acknowledges support by the Sloan and Beckman Foundations.

References and Notes

(1) Wikström, M. *Nature* **1977**, *266*, 271.
(2) Iwata, S.; Ostermeier, C.; Ludwig, B.; Michel, H. *Nature* **1995**, *376*, 660.
(3) Tsukihara, T.; Aoyama, H.; Yamashita, E.; Tomizaki, T.; Yamaguchi, H.; Shinzawa-Itoh, K.; Nakashima, R.; Yaono, R.; Yoshikawa, S. *Science* **1995**, *269*, 1069.
(4) Tsukihara, T.; Aoyama, H.; Yamashita, E.; Tomizaki, T.; Yamaguchi, H.; Shinzawa-Itoh, K.; Nakashima, R.; Yaono, R.; Yoshikawa, S. *Science* **1996**, *272*, 1136.
(5) Yoshikawa, S.; Shinzawa-Itoh, K.; Nakashima, R.; Yaono, R.; Yamashita, E.; Inoue, N.; Yao, M.; Fei, M. J.; Libeu, C. P.; Mizushima, T.; Yamaguchi, H.; Tomizaki, T.; Tsukihara, T. *Science* **1998**, *280*, 1723.
(6) Fergusson-Miller, S.; Babcock, G. T. *Chem. Rev.* **1996**, *96*, 2889.
(7) Rich, P. In *Protein Electron Transfer*; Bendall, D. S., Ed.; BIOS Scientific Publishers Ltd.: Oxford, U.K., 1996; pp 217−248.
(8) Rich, P.; Moody, A. J. In *Bioelectrochemistry*: *Principles and Practice*; Graber, P., Milazzo, G., Eds.; Birkhauser Verlag AG: Basel, 1997; pp 419−456.
(9) Papa, S., Guerrieri, F., Tager, J. M., Eds. *Frontiers of Cellular Bioenergetics: Molecular Biology, Biochemistry, and Physiopathology*; Plenum Press: New York, 1998.
(10) Kannt, A.; Lancaster, C. R. D.; Michel, H. *Biophys. J.* **1998**, *74*, 708.
(11) Lambry, J.-C.; Vos, M. H.; Martin, J.-L. *J. Phys. Chem. A* **1999**, *103*, 10132.
(12) Moore, D. B.; Martínez, T. J. *J. Phys. Chem. A* **2000**, *104*, 2367, 2525.
(13) Nagle, J. F.; Morowitz, H. J. *Proc. Natl. Acad. Sci. U.S.A.* **1978**, *75*, 298.
(14) Gutman, M.; Nachliel, E. *Biochim. Biophys. Acta* **1990**, *1015*, 391.
(15) Pomès, R.; Roux, B. *Biophys. J.* **1997**, *71*, 19.
(16) Riistama, S.; Hammer, G.; Puustinen, A.; Dyer, B. R.; Woodruff, W. H.; Wikström, M. *FEBS Lett.* **1997,** *414*, 275.
(17) Hofacker, I.; Schulten, K. *Proteins Struct. Funct. Genet.* **1998**, *30*, 100.
(18) Medvedev, D. M.; Daizadeh, I.; Stuchebrukhov, A. A. *J. Am. Chem. Soc.* **2000**, *122*, 6571.
(19) Hallén, S.; Brzezinski, P.; Malmström, B. G. *Biochemistry* **1994**, *33*, 1467.
(20) Ädelroth, P.; Brzezinski, P.; Malmström, B. G. *Biochemistry* **1995**, *34*, 2844.
(21) Ädelroth, P.; Sigurdson, H.; Hallén, S.; Brzezinski, P. *Proc. Natl. Acad. Sci. U.S.A.* **1996**, *93*, 12292.
(22) Brzezinski, P.; Ädelroth, P. *J. Bioenerg. Biomembr.* **1998**, *30*, 99.
(23) Paula, S.; Sucheta, A.; Szundi, I.; Einarsdóttir, Ó. *Biochemistry* **1999**, *38*, 3025.
(24) Jasaitis, A.; Verkhovsky, M. L.; Morgan, J. E.; Verkhovskaya, M. L.; Wikström, M. *Biochemistry* **1999**, *38*, 2697.
(25) Verkhovsky, M. L.; Morgan, J. E.; Wikström, M. *Biochemistry* **1995**, *34*, 7483.
(26) Crooks, J. E. In *Proton-Transfer Reactions*; Caldin, E., Gold, V., Eds.; Chapman and Hall: London, 1975; pp 153−177.
(27) Gutman, M.; Nachliel, E. *Biochim. Biophys. Acta* **1995**, *1231*, 123.
(28) Gutman, M.; Nachliel, E. *Annu. Rev. Phys. Chem.* **1997**, *48*, 329.
(29) Papa, S.; Capitanio, N. *J. Bioenerg. Biomembr.* **1998**, *30*, 109.
(30) Konstantinov, A. *J. Bioenerg. Biomembr.* **1998**, *30*, 121.
(31) Rich, P. R.; Jünemann, S.; Meunier, B. *J. Bioenerg. Biomembr.* **1998**, *30*, 131.
(32) Wikström, M.; Morgan, J. E.; Verkhovsky, M. *J. Bioenerg. Biomembr.* **1998**, *30*, 139.
(33) Hendler, R. W. *J. Bioenerg. Biomembr.* **1991**, *23*, 805.